Title

A Combination of Distinct Vascular Stem/Progenitor Cells for Neovascularization and Ischemic Rescue.

Journal

Arteriosclerosis, thrombosis, and vascular biology, 43(7)

ISSN

1079-5642

Authors

Zhao, Liming
Lee, Andrew S
Sasagawa, Koki
et al.

Publication Date

2023-07-01

DOI

10.1161/atvbaha.122.317943

Peer reviewed

Arteriosclerosis, Thrombosis, and Vascular Biology

TRANSLATIONAL SCIENCES

A Combination of Distinct Vascular Stem/Progenitor Cells for Neovascularization and Ischemic Rescue

Liming Zhao,* Andrew S. Lee,* Koki Sasagawa,* Jan Sokol, Yuting Wang, Ryan C. Ransom, Xin Zhao, Chao Ma, Holly M. Steininger, Lauren S. Koepke, Mimi R. Borrelli, Rachel E. Brewer, Lorene L.Y. Lee, Xianxi Huang, Thomas H. Ambrosi, Rahul Sinha, Malachia Y. Hoover, Jun Seita, Irving L. Weissman, Joseph C. Wu, Derrick C. Wan, Jun Xiao, Michael T. Longaker, Patricia K. Nguyen, Charles K.F. Chan

BACKGROUND: Peripheral vascular disease remains a leading cause of vascular morbidity and mortality worldwide despite advances in medical and surgical therapy. Besides traditional approaches, which can only restore blood flow to native arteries, an alternative approach is to enhance the growth of new vessels, thereby facilitating the physiological response to ischemia.

METHODS: The Actin^{CreER}/R26$^{VT2/GK3}$ Rainbow reporter mouse was used for unbiased in vivo survey of injury-responsive vasculogenic clonal formation. Prospective isolation and transplantation were used to determine vessel-forming capacity of different populations. Single-cell RNA-sequencing was used to characterize distinct vessel-forming populations and their interactions.

RESULTS: Two populations of distinct vascular stem/progenitor cells (VSPCs) were identified from adipose-derived mesenchymal stromal cells: VSPC1 is CD45-Ter119-Tie2+PDGFRa-CD31+CD105^{high}Sca1^{low}, which gives rise to stunted vessels (incomplete tubular structures) in a transplant setting, and VSPC2 which is CD45-Ter119-Tie2+PDGFRa+CD31-CD105^{low}Sca1^{high} and forms stunted vessels and fat. Interestingly, cotransplantation of VSPC1 and VSPC2 is required to form functional vessels that improve perfusion in the mouse hindlimb ischemia model. Similarly, VSPC1 and VSPC2 populations isolated from human adipose tissue could rescue the ischemic condition in mice.

CONCLUSIONS: These findings suggest that autologous cotransplantation of synergistic VSPCs from nonessential adipose tissue can promote neovascularization and represents a promising treatment for ischemic disease.

GRAPHIC ABSTRACT: A graphic abstract is available for this article.

Key Words: adipose tissue ■ angiogenesis ■ hindlimb ischemia ■ mesenchymal stem cells ■ neovascularization ■ peripheral vascular disease ■ stem cells

Ischemic vascular disease remains a leading cause of vascular morbidity and mortality worldwide despite advances in medical and surgical therapy.[1,2] Despite significant advances in medical and surgical treatments, traditional approaches, such as thrombectomy, angioplasty, and stenting, can only restore blood flow through native arteries, thus, limiting their utility in patients with advanced and diffuse disease. Therapeutic neovascularization, using biological agents to grow new vessels, is a promising alternative to current strategies.

See accompanying editorial on page 1278

Correspondence to: Charles K.F. Chan, 265 Campus Dr, Stanford, CA 94305, Email chazchan@stanford.edu; or Patricia K. Nguyen, 300 Pasteur Dr, Stanford, CA 94305, Email pknguyen@stanford.edu; or Michael T. Longaker, 257 Campus Dr, Stanford CA 94305, Email longaker@stanford.edu
*L. Zhao, A.S. Lee, and K. Sasagawa contributed equally to this work.
Supplemental Material is available at https://www.ahajournals.org/doi/suppl/10.1161/ATVBAHA.122.317943.
For Sources of Funding and Disclosures, see page 1275–1276.

Arterioscler Thromb Vasc Biol is available at www.ahajournals.org/journal/atvb

Nonstandard Abbreviations and Acronyms

CFP	cyan fluorescent protein
FACS	fluorescence-activated cell sorting
FGF	fibroblast growth factor
GFP	green fluorescent protein
GFR	growth factor reduced
HemSC	hemangioma stem cell
MSC	mesenchymal stromal cell
OFP	orange fluorescent protein
PBS	phosphate-buffered saline
RFP	red fluorescent protein
SMA	alpha smooth muscle actin
UMAP	uniform manifold approximation and projection
VEGF	vascular endothelial growth factor
VSPC	vascular stem/progenitor cell
VWF	von Willebrand factor

Highlights

- Two distinct vascular stem/progenitor cells (VSPCs) were identified from both mouse and human adipose-derived mesenchymal stromal cells.
- VSPC1 (CD45-Tie2+PDGFRa-CD31+CD105^{hi}Sca^{lo}) gives rise to stunted vessels.
- VSPC2 (CD45-Tie2+PDGFRa+CD31-CD105^{lo}Sca^{hi}) forms both vessels and fat.
- Cotransplantation of VSPC1 and VSPC2 is required to form functional vessels and rescue ischemic damages in vivo.

It is well known that the body has developed mechanisms to alleviate ischemia caused by atherosclerosis. The growth of blood vessels in adult organisms can occur via the development of collateral arteries (eg, arteriogenesis) or the sprouting of capillaries (eg, angiogenesis). While the former describes the remodeling of existing arteriolar connections, the latter is stimulated by acute[3] or chronic hypoxia.[4] The degree of arteriogenesis and angiogenesis, however, is inadequate to meet the demands of ischemic organs. The reasons behind this remain unclear. Perhaps some patients lack the necessary growth factors or progenitor cells to stimulate these repair systems. The administration of exogenous angiogenic factors, including VEGF (vascular endothelial growth factor),[5] FGF (fibroblast growth factor),[6] and recombinant proteins,[7] however, have been met with mixed results. Similarly, clinical trials evaluating the efficacy of various adult stem cell populations,[8,9] including bone marrow stem cells, circulating endothelial progenitor cells and adipose-derived stem cells, have shown only modest therapeutic benefits, which have been largely attributed to the paracrine effects of transplanted cells rather than reconstitution of functional vasculature by donor cell populations.[10]

Mesenchymal stromal cells (MSCs) have been viewed as a potential source for vessel progenitors.[11–13] Stromal progenitor cells are inherent to almost every organ of the human body that contains connective tissue.[11] The term mesenchymal stem cell or mesenchymal stromal cell has traditionally been applied to encompass many of these progenitor cell classes, including stromal cells derived from bone marrow, adipose tissue, and other organs.[14] Contrary to early reports, however, based on recent studies, MSCs are not a single multipotent population of cells that give rise to osteoid, adipose, endothelial,[15,16] and myogenic progeny,[14] but are composed of distinct lineage-committed cell subsets, namely specific stromal cell populations that are capable of giving rise to distinct cell fates.[15,16]

Several markers have been identified to define vessel-forming endothelial stem/progenitor cells, mostly by co-staining of the endothelial marker CD31 with fluorescence-labeled donor cells.[17,18] Although it remains challenging to identify novel progenitor cells capable of forming functional vessels that carry blood,[19–21] detection of clonal progenitor populations has been achieved through lineage tracing studies of individual cells using "Rainbow" mice,[22–24] which harbor a multicolor Cre-dependent reporter construct. To provide an unbiased in vivo survey of clonal vasculogenic activity by all potential cell types, the rainbow mice were crossed with mice carrying a ubiquitous promotor rather than specific lineage-restricted promoters.[25] Using this transgenic reporter system, we identified novel mesenchymal stromal cell subpopulations capable of forming vessels de novo.

In this study, we corroborated the presence of vessel-forming MSC populations in mice[15,16] using multicolor lineage tracing methods, identified a specific vessel-forming MSC population and a multipotent MSC population that gives rise to both fat and vessels using a unique transplantation assay, and evaluated the function of transplanted cells in vivo. Furthermore, we identified corresponding populations from human donor adipose tissue and demonstrated the ability to guide these cell populations to reconstitute functional vessels in vivo.

MATERIALS AND METHODS

The data that support the findings of this study are available from the corresponding author upon reasonable request.

Rainbow Reporter Mice

We utilized the "Rainbow" transgenic reporter mouse to evaluate clonal expansion in vessels and to determine the existence of injury-responsive cell populations. The Actin^{CreER}-R26$^{VT2/GK3}$ ("Rainbow") transgenic reporter mouse was generated by crossing the Actin^{CreER} transgenic mouse with the R26$^{VT2/GK3}$ transgenic mouse, to enable Cre-dependent cell labeling with

a 4-color reporter construct at the ROSA locus.[22,26] Tamoxifen delivery activates Cre recombinase that induces random and specific recombination, causing Cre-positive cells to express 1 of 10 possible color combinations of 4 fluorescent proteins at the ROSA locus: MSCs; CFP (cyan fluorescent protein); RFP (red fluorescent protein), or OFP (orange fluorescent protein). Actin is ubiquitously expressed, thus, tamoxifen induction of $Actin^{CreER}$/$R26^{VT2/GK3}$ allows for an unbiased in vivo survey of clonal vasculogenic activity by all potential cell types rather than specific lineage-restricted promoters. In our experiment, 8-week-old rainbow reporter mice ($Actin^{CreER+/-}$-$R26^{VT2/GK3+/+}$) were induced with tamoxifen in corn oil by gavage at the dosage of 200mg/kg per day for 1 week. Then the hindlimb ischemia surgery and sham surgery were performed. Two weeks after surgery, the vasculature structures around the ligation site were imaged and collected for histological assessment. The probability for any given adjacent cells to share the same color is 1 in 10. Further, we estimate that the probability of obtaining clones of 3 or more cells by chance is lower than or equal to (1/10)^2=1/100. We therefore chose 3 or more cells per clone for quantification because of the low likelihood of picking multiple cells of the same clone by chance. Clonal analysis was performed with Imaris software as previously described.[27] Briefly, spot-to-spot adjacency, distance tool was used to determine and spots rendering statistics tool was used to quantify clones as per the manufacturer's protocol.

Isolation and Transplantation of Mouse Adipose and Vessel-Forming Progenitors

Adult mouse adipose tissue (derived from inguinal fat pads) and lung tissue were isolated from 8- to 12-week-old male donor mice (strains are indicated in figure legends), finely minced with a razor blade, and digested in collagenase digest buffer (2.2 mg/mL Collagenase II [Sigma] supplemented with 100 U/mL DNase [Worthington] in M199 Media [Sigma]) at 37 °C for 30 minutes under constant agitation. All dissociated cells were filtered through 70-micron nylon mesh, pelleted at 400 g at 4 °C for 5 minutes, resuspended in fluorescence-activated cell sorting (FACS) buffer (2% FBS in phosphate-buffered saline [PBS]), blocked with rat IgG, and stained with fluorochrome-conjugated antibodies against mouse CD45, Ter119, Tie2, Sca1, CD105, PDGFRα, and CD31. The stained cells were then sorted on the BD Aria II Flow Cytometer. Compensation, fluorescence minus one controls, and unstained cells were utilized to adjust the gating appropriately. Two hundred thousand sorted vessel-forming progenitors were pelleted by centrifugation, resuspended in 2 µL of Matrigel, and injected underneath the inguinal fat pads of 8- to 12-week-old immunodeficient Rag2/gamma(c) knockout male mice to investigate the angiogenesis potential in vivo. In ischemic rescue studies, 500 000 sorted vessel-forming progenitors were resuspended in 2 µL of growth factor reduced (GFR) Matrigel and injected around ligated femoral artery of 8 to 12 weeks old immunodeficient Rag2/gamma(c) knockout male mice. Only male mice were used in our study to avoid the effect of estrogen variation on angiogenesis.[28–30]

Single-Cell RNA-Sequencing by 10X Genomics and Data Processing

Single cells were isolated by their specific markers via FACS. Single cell libraries were prepared following the user guide for Chromium Next GEM Single Cell 3′ Reagent Kits v3.1 (Dual Index) from 10X Genomics (10x Genomics Inc San Francisco, CA). The prepared libraries were sequenced by HiSeq 4000 platform with 150 bp paired end reads. Sequencing data were then uploaded to Gene Expression Omnibus.

Single-cell sequencing data were then processed and analyzed with "Seurat" R package (V3.1.4).[31] For sequencing data quality control, all samples were filtered to remove low-quality cells with very few genes (minimum of 300 genes) and weakly expressed genes (<5 cells). Samples were further filtered using a maximum RNA count of 15 000 and a maximum mitochondrial proportion of 22% for mouse vessel-forming progenitor cells. The mitochondrial cutoff was determined by the extreme outlier value (upper quartile+3×IQR) of mitochondrial transcriptome proportions for each group's entire cell population. The minimum gene count helped remove low-quality or empty droplets, while the maximum RNA count excluded potential multiplets. Last, the mitochondrial transcriptome cutoff removed dying cells with weaker biological signals. After these quality checks, all samples were combined without applying any batch correction, as they were processed and sequenced in the same batch and with the same condition. Standard log normalization and scaling of read counts were applied. Principal component analysis (PCA) was applied to the entire cell population for both samples, selecting the 30 most variable components. Cells were then embedded into a K-nearest neighbor graph using the "FindNeighbors" function that works on the euclidean distance in PCA space. Subsequently, vessel-forming progenitor cells were partitioned into clusters using the Leiden algorithm. Last, uniform manifold approximation and projection was used to visualize the cells in 2 dimensions.

To determine all possible ligand-receptor interactions between our target populations, we utilized the "CellChat" R package that draws on a manually curated database of literature-supported ligand-receptor interactions called "CellChatDB."[32] To run this analysis, significantly over-expressed ligands and receptors in each of our target populations were first estimated. Next, each ligand-receptor interaction was assigned with a probability based on gene expression levels and prior known knowledge of signaling ligands, their receptors and cofactors. Autocrine interactions were also considered.

Isolation and Transplantation of Human Vessel-Forming Progenitors From Adipose Tissue

Human adipose lipoaspirates were obtained after informed consent from female patients (26–54 years old). Fresh lipoaspirates were separated from blood, and lipoaspiration fluid were passed through a 100 µm nylon mesh. Solid matter was then resuspended in collagenase digest buffer (2.2 mg/mL Collagenase II [Sigma] supplemented with 100 U/mL DNase [Worthington] in M199 Media [Sigma]), shaken in CERTOMAT BS-1 Incubation-Shaking Cabinet at 37 °C for 30 minutes, sedimented on Histopaque-1119 Density gradient to remove blood and dead cells, washed, and pelleted at 400×*g* at 4 °C. Cells were then plated on Lonza Endothelial Growth Media and transduced with CMV-GFP expressing lentivirus. Twenty-four hours after transduction, cells were lifted with collagenase, resuspended in staining media (2% FBS in PBS), blocked with rat IgG, and stained with fluorochrome-conjugated antibodies against human CD45, Tie2, PDGFRα, and CD31 for FACS on

the BD Aria II Flow Cytometer. As with mouse samples, the gating was adjusted based on compensation, fluorescence minus one controls and, unstained cells. In ischemic rescue studies, 500 000 sorted VSPC1+VSPC2 vessel-forming progenitors were injected around ligated femoral artery of 8- to 12-week-old immunodeficient Rag2/gamma(c) knockout male mice.

Histological Analysis of Blood Vessel Perfusion With Lectin

Recipient 8- to 12-week-old immunodeficient Rag2/gamma(c) knockout male mice were briefly anesthetized with Isoflurane and then injected intravenously with 100 µL of DyLight 649-labeled Tomato Lectin (Vector Labs). Ten minutes after injection, mice were fully anesthetized with tribromoethanol (125–250 mg/kg body weight). Mice were then sacrificed and perfused with 10 mM EDTA in PBS to remove peripheral blood by accessing the left ventricle through an incision in the thoracic cavity. Incisions were also made to access engrafted areas that were then imaged with a Leica DMI6000B inverted microscope system. Engrafted areas were then fully excised, fixed in 4% paraformaldehyde at 4 °C overnight, and whole-mounts were prepared for confocal imaging using the Zeiss LSM-TPMT 800.

Lentivirus Production and Transduction of Human Adipose Cells

HEK 293T cells (System Biosciences, Mountain View, CA) were plated at 50% confluency on 10 cm dishes and transfected with 12 µg of a construct expressing Actin-GFP, 8 µg of packaging Ppax2, and 4 µg of VSVG plasmids using Lipofectamine 2000 (Invitrogen) as per the manufacturer's instructions. Supernatant was collected 24 and 48 hours after transfection, filtered through a 0.45-µm pore-size cellulose acetate filter (Millipore, Billerica, MA), and mixed with PEG-it Virus Concentration Solution (System Biosciences) overnight at 4 °C. Viruses were precipitated at 1500×*g* at 4 °C the next day and resuspended in PBS. Digested human lipoaspirate cells were infected with virus overnight for 24 hours prior to sorting for VSPC1 and VSPC2 markers and xeno-transplantation into 8- to 12-week-old immunodeficient Rag2/gamma(c) knockout male mice.

Immunofluorescence Microscopy

Immunofluorescence on specimens was performed using an M.O.M. immunodetection kit from Vector Laboratories according to manufacturer's instructions. Briefly, specimens were fixed in 2% PFA at 4 °C overnight, treated with a blocking reagent, and then probed with Alexa-dye conjugated antibodies at 4 °C overnight. Isotype control antibodies were used for negative controls. Specimens were next washed with PBS, and then coverslips were then applied. Slides were imaged with a Zeiss LSM710 or LSM980 confocal microscope.

Gene Expression

Microarray analyses were performed on highly purified, double-sorted mouse populations of (VSPC1, CD45$^-$ Tie2$^+$ CD105^{high} PDGFRα$^-$ CD31$^+$) and P2 (VSPC2, CD45$^-$ Tie2$^+$ CD105^{lo} PDGFRα$^+$ CD31$^-$). Each population was sorted in 3 independent sorts using cells isolated from 8-week-old mice. RNA was isolated with RNeasy Micro Kit (Qiagen, Germantown, MD) as per manufacturer's instructions. RNA was twice amplified with a RiboAmp RNA amplification kit (Arcturus Engineering, Mountain View, CA). Amplified cDNA was streptavidin-labeled, fragmented, and hybridized to Affymetrix 430-2.0 arrays as recommended by the manufacturer (Affymetrix, Santa Clara). Arrays were scanned with a Gene Chip Scanner 3000 (Affymetrix) running GCOS 1.1.1. software. Raw microarray data were submitted to Gene Expression Commons (https://gexc.riken.jp),[33] where data normalization was computed against the Common Reference, which is a large collection (n=11 939) of publicly available microarray data from the National Center for Biotechnology Information Gene Expression Omnibus (NCBI GEO). Meta-analysis of the Common Reference also provided the dynamic range of each probe set on the array, and, in situations where there are multiple probe sets for the same gene, the probe set with the widest dynamic range was used for analysis. The Affymetrix Mouse Genome 430 2.0 Array included 45 101 probe sets, of which 17 872 annotated genes were measurable. Heat maps representing fold change of gene expression were generated in Gene Expression Commons.

Hindlimb Ischemia Model

Hindlimb ischemia was performed in 8- to 12-week-old immunodeficient Rag2/gamma(c) knockout male mice, as previously described.[34] Mice were anesthetized with 1.5% isoflurane, and the right hindlimb was opened to expose the femoral artery for ligation, after which, a total number of 500 000 VSPC1, VSPC2, or VSPC1+VSPC2 cells (1:1 ratio) suspended in 2 µL GFR Matrigel were delivered around ligated femoral artery for studies to restore blood flow following injury. Control animals received 2 µL GFR Matrigel containing GFR Matrigel alone as indicated in figure legends. The skin was closed using 6-0 silk sutures. Revascularization was monitored by laser Doppler perfusion imaging.

Measurement of Blood Flow by Laser Doppler Imaging

Following ligation of the right femoral artery, laser Doppler perfusion imaging was used to assess revascularization. Animals were anesthetized using 1.5% isoflurane in oxygen, and hindlimb vascularization was monitored by laser Doppler perfusion imaging using a PeriScan PIM3 laser Doppler system (Perimed AB, Sweden) as previously described.[34] Temperature was maintained at constant levels by keeping animals on heating pads set to 37 °C during measurement. Nonligated contralateral hindlimbs served as controls. Perfusion was calculated as the ratio of the flow in the ischemic to control limbs.

Animal Care

Actin^{CreER}/R26VT2/GK3 mice, C57BL/6J strain mice, immunodeficient Rag2/gamma(c) knockout mice, Actin-GFP and Actin-RFP reporter mice were derived and maintained in our laboratory. All animals were housed in Stanford University Laboratory Animal Facility following Stanford Animal Care and Use Committee and National Institutes of Health guidelines. Food (2018 Teklad Global 18% Protein Rodent Diet from Inotiv) and water were provided to all animals free of access by Stanford Veterinary Service Center.

Study Approval

Human adipose lipoaspirates were obtained according to the Stanford Administrative Panel on Human Subjects Research and Institutional Review Board (IRB)-approved protocols with informed consent. All animal experiments in this study were approved by the Stanford Administrative Panel on Laboratory Animal Care.

Statistical Analysis

All statistical analyses were performed with GraphPad Prism 9. Data were tested for normality by the Shapiro-Wilk test and equal variance by the *F* test. For data that passed normality and equal variance tests, statistical differences were determined using the 1-way ANOVA (Figure 3L and 3M) or repeated measures ANOVA (Figures 3I and 5E) followed by the Dunnett's post-hoc test, with α set to 0.05 for significance. The Poisson regression model was used to compare count data after the overdispersion test (Figure 1C, 1E, 1F). The Mann-Whitney test was used for data that failed either normality or equal variance test (Figure S5B). Unless specified, data are expressed as average±SEM. Sample sizes were indicated in figure legends.

Data Availability

Single-cell RNA-sequencing data have been deposited in GEO under accession code GSE181177. Microarray data is accessible with https://gexc.riken.jp/models/2548. Datasets Generated: Vessel-Forming Mesenchymal Stromal Cell Populations: Koki Sasagawa, Liming Zhao, Charles K.F. Chan, 2021, https://www.ncbi.nlm.nih.gov/geo/query/acc.cgi?acc=GSE181177, NCBI Gene Expression Omnibus, GSE181177; Vessel-Forming Mesenchymal Stromal Cell Populations model: Charles K.F. Chan, Liming Zhao, Andrew S. Lee, 2021, https://gexc.riken.jp/models/2548, gexc.riken.jp/models/2548.

RESULTS

Identification of Distinct Ischemic-Responsive Vessel-Forming Populations

It is known that tissue ischemia could stimulate a vasculogenic response including the formation of corollary vessels. We reasoned that these new vessels might be derived from either a local source or recruited from a distant source of vessel stem progenitor cells. To better understand the vasculogenic activity as a regenerative response, we induced ischemic injury in the "Rainbow" reporter mouse as previously described,[22,26] to evaluate clonal expansion in vessels and determine whether injury-responsive populations exist. The "Rainbow" reporter mouse was generated by crossing Actin^{CreER} transgenic mouse with R26$^{VT2/GK3}$ transgenic mouse, to enable Cre-dependent unbiased labeling with a four-color reporter construct at the *ROSA* locus (Figure 1A). Tamoxifen delivery activates Cre recombinase that induces random and specific recombination, causing Cre-positive cells to express 1 of 10 possible color combinations of 4 fluorescent proteins at the *ROSA* locus: GFP (green fluorescent protein); CFP (cyan fluorescent protein); RFP (red fluorescent protein), or OFP. Actin is ubiquitously expressed, thus, tamoxifen induction of Actin^{CreER}/R26$^{VT2/GK3}$ following ischemic injury allows for an unbiased in vivo survey of clonal vasculogenic activity by all potential cell types rather than specific lineage-restricted promoters, such as VE-CadherinER or Nestin-CreER.

We observed that femoral artery ligation stimulated the formation of patent collateral blood vessels within 2 weeks of ligation, indicated by the increased number of vessel branches from femoral artery (Figure 1B and 1C). The formation of these vessels also involved the clonal expansion of vessel-forming cells as detected by tracing of Rainbow-labeled tissue with confocal microscopy (Figure 1D). We then quantified the frequency of contiguous clonally labeled cells in vessels with comparable diameters from both sham and ischemic Rainbow tissues. We determined that whilst there was no significant difference in the number of clones (Figure 1E), the number of cells per clone was significantly greater in the ischemic compared with non-ischemic tissue (Figure 1F). These findings are consistent with previous observations,[35,36] suggesting that endogenous vessel-forming progenitor populations are responsive to ischemic injury and could contribute to neovascularization. However, severe ischemia, resulting from acute arterial occlusion could outstrip the capacity of local vessel-forming progenitors to regenerate vessels, as the frequency of the endogenous vasculogenic population may not be sufficient to adequately respond to acute ischemic damage. This prompted us to identify the specific vessel-forming progenitor cells for their prospective isolation and to determine if there may be additional sources of these vessel-forming progenitors that could be rapidly isolated for transplantation to rescue ischemia in tissues.

To identify a transcriptomic signature associated with ischemia, we checked publicly available single-cell RNA sequencing datasets with similar experimental parameters to our ischemia model. Although this data is not publicly available in the hindlimb ischemia model, it was available for ischemic hearts days 3 and 7 post-sham or myocardial infarction surgeries.[37] Given the data compares cell populations in tissue that emerge before and after ischemic tissue injury, analyzing these single-cell transcriptomic datasets provide important clues for identifying injury-responsive vascular progenitors. To enrich for cells relevant to ischemic injury and repair, we excluded cells of the atria, annulus fibrosus, and atrioventricular valves. Forty-two distinct clusters were identified and showed dynamic change after ischemic injury. Based on their cell surface markers, these clusters can be grouped into 3 major populations represented by Pecam1+ (encoding CD31), Pdgfra+ (encoding PDGFRa), and Ptprc+ (encoding CD45) populations (Figure S1A through S1D). To test the functionality of these populations, we isolated these populations (CD31+,

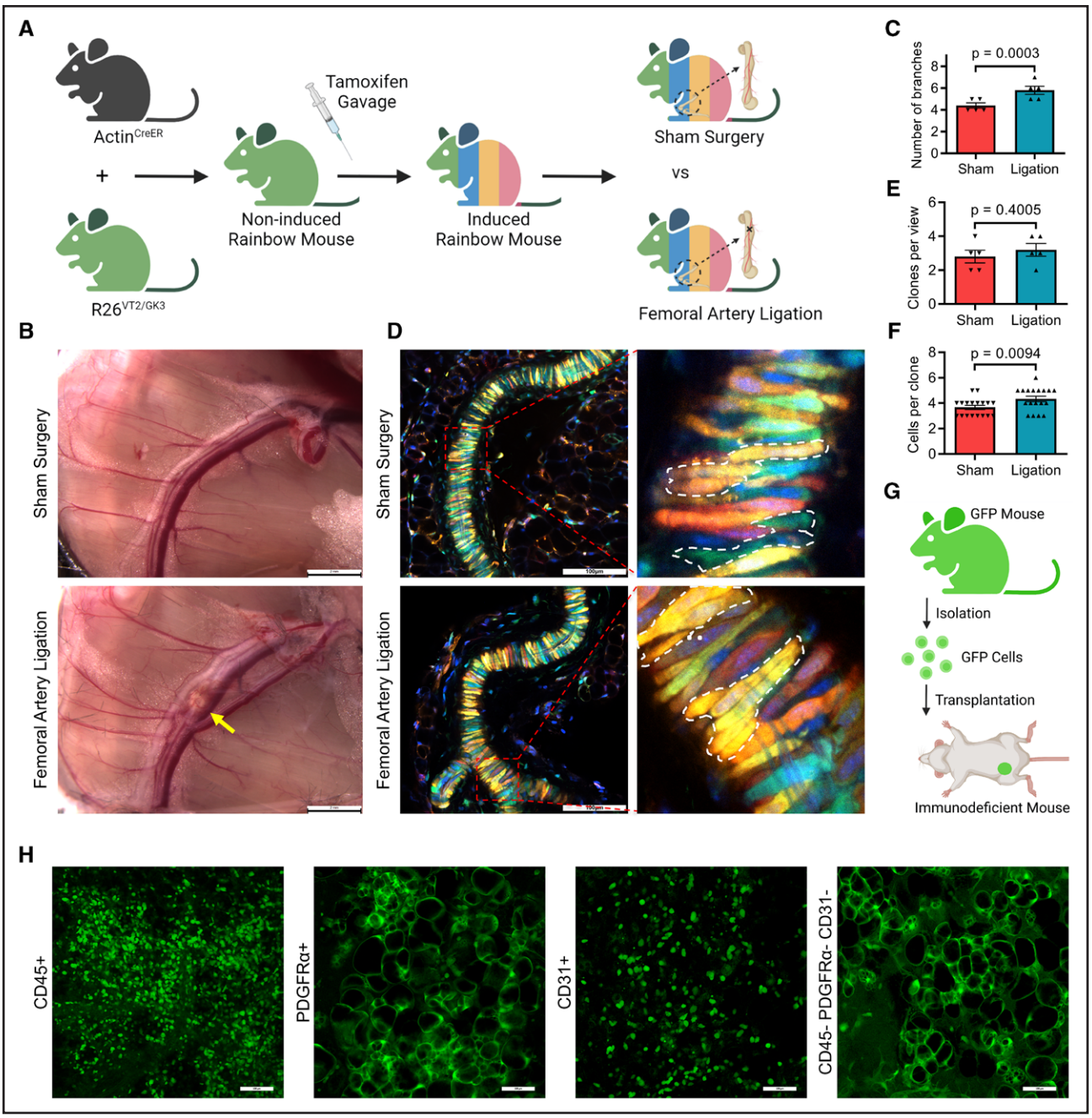

Figure 1. Clonal analysis of ischemia-responsive progenitor activity in vivo.
A, Schematic diagram of the Actin-Cre rainbow reporter system utilized for clonal analysis. Diagram was created with Biorender. **B**, Bright field images of non-ischemic (sham surgery) and ischemic (femoral artery ligation) hindlimbs 2 weeks post-surgery. The yellow arrow indicates the ligation site. Scale bars=2 mm. **C**, The number of vessel branches from the femoral artery was visually quantified under bright field microscopy (n=5). **D**, Confocal whole-mount micrographs of non-ischemic (sham surgery) and ischemic (femoral artery ligation) vessels of induced rainbow mice 2 weeks post-ligation. The white dash lines circled clones. Scale bars=100 μm. **E**, A bar graph comparing the number of clones in non-ischemic (sham surgery, n=5) and ischemic (femoral artery ligation, n=5) hindlimb vessels. **F**, A bar graph comparing the number of cells per clone in non-ischemic (sham surgery, n=20 clones) and ischemic (femoral artery ligation, n=20 clones) hindlimb vessels. **G**, Schematic diagram of cell transplantation. Cells were isolated from GFP donor mice adipose tissue by fluorescence-activated cell sorting (FACS) and transplanted into the inguinal fat pad of immunodeficient Rag2/gamma(c) knockout mice. Diagram was created with www.Biorender.com. **H**, Differentiation potential of different cell populations after transplantation into inguinal fat pads of immunodeficient Rag2/gamma(c) knockout mice. Scale bars=100 μm.

PDGFRa+ or CD45+) separately with FACS from adipose tissue of Actin-GFP mice, which express GFP in every cell of the body, then transplanted into the inguinal fat pads of immunodeficient Rag2/gamma(c) knockout mice (Figure 1G). Two weeks after transplantation, GFP-positive grafts were dissected and imaged to determine

the differentiation capacities, but none of them could give rise to vessels (Figure 1I). Donor cells derived GFP signals have been confirmed by immunostaining (Figure S2).

We have previously observed that dissociated mouse MSCs could be subfractionated based on differential expression of Tie2, CD51, and CD45 into functionally distinct subsets.[14] While CD45 donor cells primarily gave rise to blood lineages, and CD51-positive cells produced bone, transplanted Tie2 positive cells generated adipocytes and vessels.[14] Analysis of the differentially expressed genes of 42 distinct clusters also revealed that Tek (the gene encoding Tie2) could be used as a marker to further distinguish these populations (Figure S1E). We then transplanted and tested Tie2+ and Tie2− subpopulations of CD31+, PDGFRa+ or CD45+ populations. We found that transplantation of PDGFRa+Tie2+ population gave rise to stunted vessels and adipocytes, whereas transplantation of the CD31+Tie2+ population gave rise to only stunted vessels (Figure 2A).

Comparison of MSCs Tie2+ Subpopulations

Numerous studies, including several clinical trials in patients, have suggested that pools of MSCs residing within bone marrow and adipose tissue could be harvested and transplanted for efficacious rescue of acute ischemic damage caused by cardiac arrest or stroke.[38–40] While there are some claims of remarkable improvement after MSC transplantation, the evidence base is weak and a mechanistic basis for ischemic rescue in these instances remains unclear. Some studies attribute the improvement to contribution of new vessel formation by transplanted MSCs, while others suggest that paracrine signaling by transplanted MSCs was the major factor.[10] In addition, there are also reports that MSC populations are highly heterogeneous and may be interspersed with non-MSC populations,[15,16] suggesting that some MSC populations may be more suitable for rescue of ischemic damage than others.

To uncover the precise roles that transplanted MSCs perform in an ischemic environment, we endeavored to prospectively isolate MSC populations from adipose tissue that exhibit vessel-forming activity. We then tested CD31+ Tie2+ and PDGFRa+Tie2+ populations with a panel of MSC markers including CD45, CD105, and Sca1 to determine if these proteins are differentially expressed amongst Tie2(+) vessel-forming MSCs. We found that differential expression of these markers subfractionated Tie2(+) populations into 2 main populations that appeared to be 2 distinct populations of vessel-forming MSCs: CD45-Ter119-Tie2+PDGFRα-CD31+CD105^{high}Sca1^{low} (referred to as "P1") and CD45-Ter119-Tie2+PDGFRα+CD31-CD105^{low}Sca1^{high} (referred to as "P2"; Figure 2B; Figure S3). P1 transplanted into the inguinal fat pads in Matrigel formed stunted vessels while P2 formed both vessels and adipose tissue (Figure 2C and 2D). These results indicate that formation of de novo vessels could be a mechanism through by which transplanted MSCs ameliorate ischemic damage.

Given that P2 vasculogenic MSCs generated adipocytes in addition to vessels in vivo, we investigated whether this adipogenic potential was unique to P2 MSCs from adipose tissues. We isolated P2 MSCs from Actin-GFP donor mice lungs, a relatively fat-absent tissue, to confirm whether adipocytes evident in grafted sites were independent of the tissue source of donor P2 cells and were not the result of contaminating adipose tissue. Indeed, P2 MSCs from the pulmonary tissue also gave rise to fat and vessel structures in a manner identical to adipose-derived MSCs, when transplanted into the inguinal fat pads of recipient animals. Adipocytes derived from lung P2 populations have been confirmed by adipocyte marker Perilipin 1 (Figure 2E). Taken together, these results suggest that P2 MSCs are multipotent and able to differentiate into fat and vessels, while P1 is restricted to vessel formation.

P1 and P2 Populations Are Vascular Stem/Progenitor Cells

To assess the proliferative and self-renewal capabilities of our isolated P1 and P2 populations, we performed colony-forming assays. Populations isolated by FACS from a noninduced rainbow mouse were transplanted into the inguinal fat pads of separate immunodeficient Rag2/gamma(c) knockout mice or performed in vitro culture to assess clonal potential (Figure S4A). Recipient mice were then pulsed with Tamoxifen. The P1 population, as previously seen, generated vessel-like structures, which appear to be produced by a single blue clone. The P2 population produced adipocyte structures that appeared to be derived from several clones of differing colors (Figure S4B). After 1 week of in vitro clone formation, P1 and P2 cells were analyzed by FACS to assess their self-renewal capabilities. 80% daughter cells of P1 (Tie2+PDGFRα-CD31+) showed Tie2+PDGFRα- phenotype and 47.4% of those cells were CD31+ (Figure S4C). Daughter cells (59.3%) of P2 (Tie2+PDGFRα+CD31−) showed Tie2+PDGFRα+ phenotype, and 99.8% of those cells were CD31− (Figure S4D). These data indicate that P1 and P2 populations are vessel-forming vascular stem/progenitor cells (VSPCs) progenitors. Henceforth, we will also refer to P1 and P2 as VSPC1 and VSPC2, respectively.

Cotransplantation of VSPC1 (P1) and VSPC2 (P2) Leads to the Development of Functional Vessels

Of the tested donor tissues, adipose tissue is the most easily accessible, abundant, and clinically suitable for autologous cell-based therapy for ischemia. Given this translational

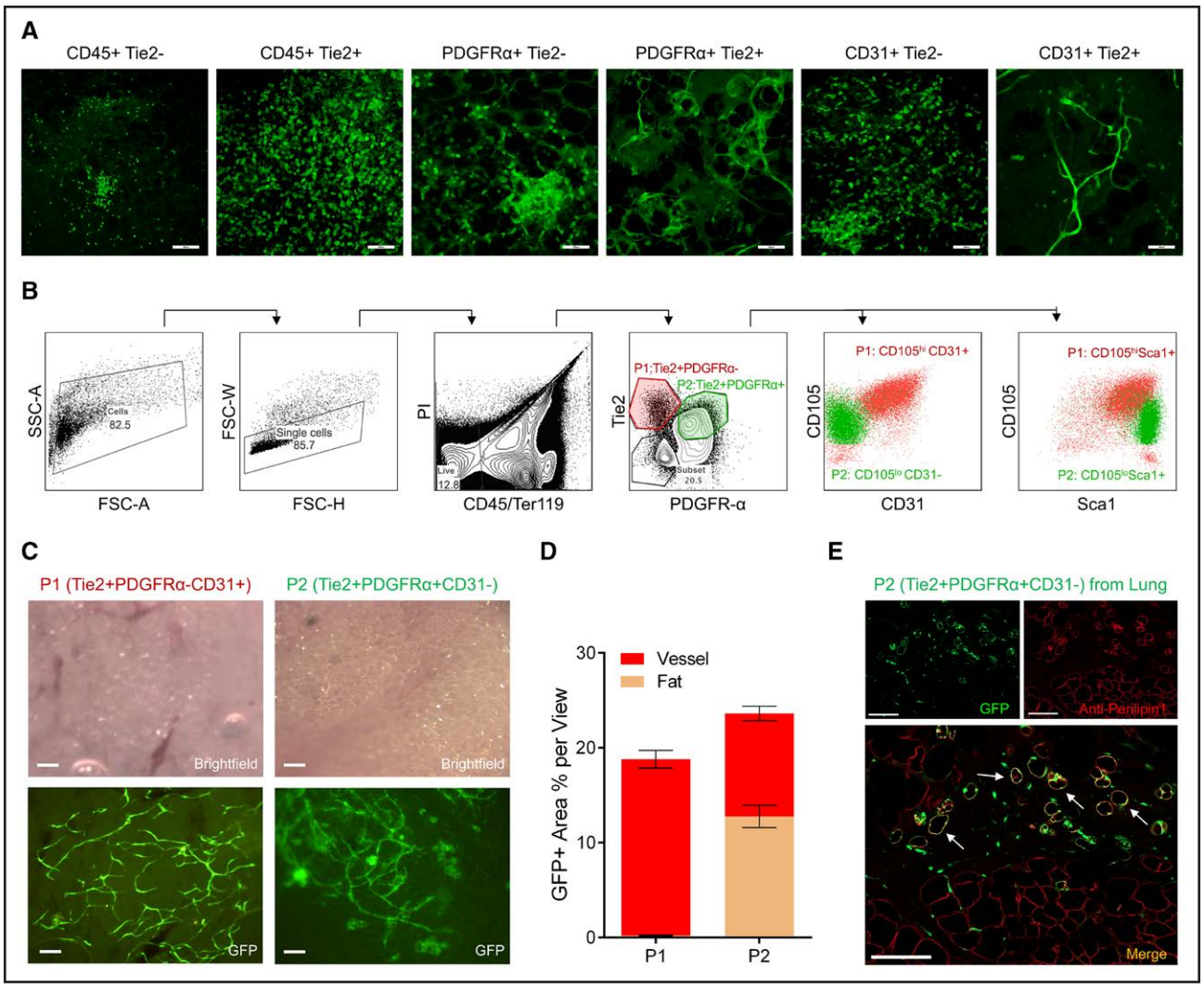

Figure 2. Cell surface markers that define vessel-forming progenitor populations.
A, Differentiation potential of different cell populations after transplantation into inguinal fat pads of immunodeficient Rag2/gamma(c) knockout mice. Scale bars=100 μm. **B**, Prospective isolation of vessel-forming progenitors by fluorescence-activated cell sorting, P1 (CD45−, Ter119−, Tie2+, CD31+, PDGFRα−, CD105^{high}, Sca-1^{low}) and P2 (CD45−, Ter119-, Tie2+, CD31−, PDGFRα+, CD105^{low}, Sca-1^{high}). **C**, Two weeks post-transplantation of P1 or P2 from adipose tissue into inguinal fat pads of immunodeficient Rag2/gamma(c) knockout mice. Scale bars=100 μm. **D**, A bar graph comparing P1 and P2 differentiation potential after transplantation. **E**, Two weeks post-transplantation of P2 from pulmonary tissue into inguinal fat pads of immunodeficient Rag2/gamma(c) knockout mice. Arrows indicate positive co-staining of Perilipin1 and GFP (green fluorescent protein). Scale bars=100 μm.

component, our subsequent experiments focused on understanding and optimizing the vessel-forming capacity of VSPC1 and VSPC2 in adipose-derived MSCs. To better understand the relationship between VSPC1 and VSPC2, we isolated both populations from the adipose tissue of Actin-GFP donor mice and cotransplanted them into the inguinal fat pads of immunodeficient Rag2/gamma(c) knockout mice. Surprisingly, the explanted grafts derived from VSPC1 and VSPC2 cotransplantation primarily contained vessel structures with minimal presence of adipose cells, and numerous GFP-labeled donor cells derived vessels were overlapped with blood flow (Figure 3A). Retro-orbital perfusion of animals with DyLight 649-lectin dye, which adheres specifically to endothelial linings of recipient mice, showed binding within donor-derived GFP vessels, demonstrating that donor cell-derived vessels were connected to host vasculature (Figure 3B). Those vessels were also stained positive for endothelial markers including CD31 and VWF (Von Willebrand factor; Figure 3C and 3D).

To determine whether the functional vessels observed following cotransplantation of the subfractionated stromal cells arose from both VSPC1 or VSPC2 donor populations, we isolated each population individually from Actin-RFP and Actin-GFP reporter mice. Single population of Actin-RFP VSPC1 cells formed stunted vessels, whereas VSPC2 cells derived from Actin-GFP reporter mice formed both stunted vessels and fat when

transplanted within the inguinal fat pads, confirming our previous observations. In contrast, cotransplantation of RFP VSPC1 cells with GFP VSPC2 cells into the inguinal fat pads of immunodeficient Rag2/gamma(c) knockout mice gave rise to functional vessels derived from both the RFP and GFP cells, as well as minimal fat (Figure 3E and 3F). These findings suggest that the combination of VSPC1 and VSPC2 MSCs has a superior effect in generating vessels while simultaneously suppressing the inclination toward adipocyte differentiation by VSPC2.

VSPC1 (P1) and VSPC2 (P2) Cotransplantation Successfully Rescues Vascularization After Femoral Artery Ligation

We next aimed to determine whether a combination of VSPC1 and VSPC2 adipose-derived MSCs could restore functional deficits in a mouse model of hind limb ischemia. VSPC1 and VSPC2 were injected as individual cells, or as cotransplants, and compared with injection of carrier only GFR Matrigel. Blood flow was monitored following ligation of the femoral artery using laser Doppler imaging (Figure 3G). Mice injected with GFR Matrigel had low levels of revascularization presumably due to the modest endogenous response to ischemic injury. In sharp contrast, injection of combined VSPC1 and VSPC2 progenitor cells significantly improved limb perfusion at 7 days post-transplantation, and this effect was enhanced at 14 and 28 days post-transplantation. There was also a significantly increased blood perfusion in VSPC1 and VSPC2 cotransplanted mice compared with mice transplanted with either VSPC1 or VSPC2 alone. The superior blood perfusion of cotransplantation lasted 28 days post-transplantation and demonstrated longevity of de novo structures formed (Figure 3H and 3I). Functional recovery observed by Doppler imaging suggests that recovery post grafts is mediated by the de novo formation of functional GFP vessels, which anastomosed with host vasculature and revascularized the site of injury (Figure 3J through 3M). Taken together, these findings indicate that cotransplantation of VSPC1 and VSPC2 cells leads to optimized neovascularization.

Regulatory Crosstalk Between VSPC1 (P1) and VSPC2 (P2) in the Promotion of Neovascularization

To further characterize VSPC1 and VSPC2 progenitor populations and determine a signaling basis for how interactions between them may guide the formation of vessels, we performed single-cell sequencing on VSPC1 and VSPC2 populations derived from mouse adipose and lung tissue using 10x Genomics Chromium platform (Figure 4A and 4B). VSPC1 and VSPC2 populations from adipose and lung tissues clustered separately based on their own cell types and tissue sources, indicating relative homogeneity of these populations (Figure 4A). Differentially expressed gene analysis confirmed the presence of a combination of cell surface markers that were used to isolate VSPC1 and VSPC2 populations (Figure 4B).

To investigate VSPC1 and VSPC2 population interaction networks, we performed CellChat analysis based on receptor-ligand interactions between the VSPC1 and VSPC2 cell populations with single-cell RNA-expression data. CellChat interaction network analysis revealed complex signaling regulation of VSPC1 to VSPC2 populations, including PDGF, CXCL12, COL4, and other signals (Figure 4C and 4D). Our previous microarray analysis of VSPC1 and VSPC2 populations from adipose, lung, and bone marrow also highlighted that PDGFβ ligand is only expressed in the VSPC1 population but not the VSPC2 population. In contrast, the receptor for PDGFβ, PDGFRα is only expressed in the VSPC2 but not the VSPC1 population (Figure 4E). These data suggest that PDGF signals may act as unidirectional stromal cues from the VSPC1 sub-fraction to guide VSPC2 progenitor cells to form vessels. This concurs with other studies which have demonstrated a critical role for PDGF in the regulation of vessel development.[41] In addition, previous studies have identified adipose-derived progenitor cells expressing PDGFRβ in the stromal vascular fraction of adipose tissue.[42]

To further explore the role of PDGF signaling in vessel formation within VSPC1 and VSPC2 cell populations, we cotransplanted VSPC1 and VSPC2 cells isolated from Actin-GFP reporter mice in Matrigel with or without a saturating dose of a PDGFR antagonist (a neutralizing antibody against PDGFRα). The presence of a PDGFR antagonist led to complete ablation of functional vessel formation. Retained GFP cells were instead characterized by a nondescript appearance and were negative for markers of endothelial (CD31), smooth muscle (alpha SMA [smooth muscle actin]), or pericyte origin (neural glial antigen 2; Figure 4F and 4G). To test if PDGF signal is specifically regulating VSPC2 cells, we also transplanted VSPC1 cells with or without PDGFR antagonist, the results showed that the inhibition of PDGF signal does not affect the function of VSPC1 cells (Figure S5A and S5B). Taken together, these findings confirm that PDGF is a key mediator of vessel formation due to its effects on VSPC1 and VSPC2 populations.

Human Lipoaspirate Contains Functional, Analogous VSPC1 (P1) and VSPC2 (P2) Populations

The successful in vivo generation of ischemia-rescuing vessels from cotransplantation of mouse VSPC1 and VSPC2 prompted us to determine whether analogous

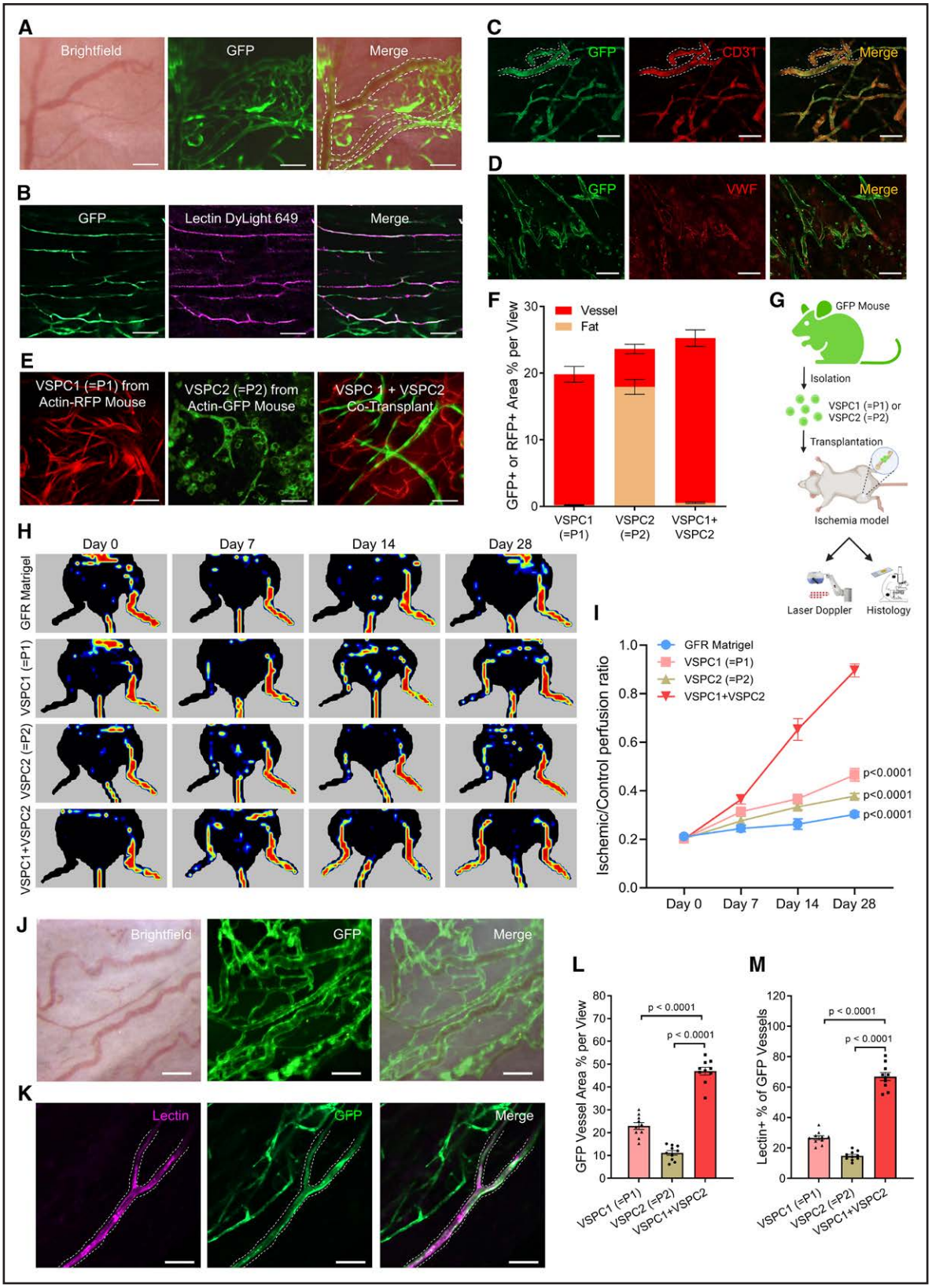

Figure 3. Cotransplantation of VSPC1 (P1) and VSPC2 (P2) populations leads to the development of functional vessels and rescue of ischemic injury.

A, Cotransplantation of 200 000 Actin-GFP (green fluorescent protein) mice derived VSPC1 and VSPC2 cell populations (1:1 ratio) in vivo (n=5). Scale bars=100 μm. **B**, Perfusion of recipient animals with DyLight 649-lectin to label vessels connected to vasculature system (n=5). Scale bars=100 μm. **C**, Immunofluorescence staining of CD31. From left to right, GFP signal from transplanted cells, (*Continued*)

cell types also exist in human stromal tissues. We analyzed published single-cell sequencing datasets of human adipose stromal vascular fraction and identified transcriptionally similar cell subsets that correspondingly express similar cell surface markers as mouse VSPC1 and VSPC2 including Tie2, PDGFRα, and CD31[43] (Figure 5A and 5B). We then assessed the stromal fraction of human abdominal lipoaspirate, which corresponds to the inguinal fat pads isolated from mice, the original tissue of origin of VSPC1 and VSPC2 cells. FACS analysis of human lipoaspirate contained both VSPC1 CD45-Tie2+PDGFRα-CD31+ and VSPC2 CD45-Tie2+PDGFRα+CD31− populations (Figure 5C). To determine whether these populations were capable of giving rise to vessels in vivo and ameliorating ischemic injury, we delivered the VSPC1 and VSPC2 populations separately or in combination into a xenotransplant model of hind limb ischemia using immunodeficient Rag2/gamma(c) knockout mice. Laser Doppler revealed significantly enhanced revascularization in animals receiving the combination of human VSPC1 and VSPC2 cells compared with controls that received carrier only (GFR Matrigel) or carrier plus VSPC1 or VSPC2 cells alone (Figure 5D and 5E). Before delivery, transplanted VSPC1 and VSPC2 cells were transduced with a GFP reporter lentivirus followed by co-staining of explanted grafts for human CD31, which revealed that donor human cells formed endothelial cells within the transplants (Figure 5F). These data indicate that human VSPC1 and VSPC2 are functionally homologous to mouse VSPC1 and VSPC2 in their ability to form vessels in an ischemic setting.

DISCUSSION

To date, efforts to regrow vessels in tissues damaged by inadequate blood supply have been met with limited success. Identifying a source of vessel-forming progenitor cells would also provide a novel strategy to rescue ischemic tissues in patients with atherosclerosis or avascular necrosis. MSCs provide a reliable and practical source of progenitor cells.[44] However, MSCs have been used in many clinical trials but have achieved mixed efficacy likely due to the heterogeneity of transplanted cells.[45] Controversy remains over whether these cells exert a paracrine effect on host tissue or are capable of forming vessels in vivo. In this study, we demonstrated that endogenous MSCs could form vessels in response to ischemia using a multicolor lineage tracing reporter system. We identified 2 distinct MSC subpopulations expressing Tie2 with vasculogenic potential VSPC1 and VSPC2 and followed their fates longitudinally using a unique transplantation assay that distinguished donor from recipient tissues. Cotransplantation of these subpopulations formed functional vessels and effectively revascularized ischemic tissue in a murine model of hind limb ischemia. We identified PDGF as critical signal involved in cell-to-cell signaling during vasculogenesis. In addition, we identified the functionally homologous MSC derived VSPC1 and VSPC2 subpopulations in humans, which can serve as a promising therapy for patients with cardiovascular and ischemic disease (Figure 5G).

Although MSCs have been touted for their multipotent potential, evidence for trans-differentiation into endothelial cell lineages in vivo is conflicting. Using genetic fate map techniques, Ubil et al[46] first reported that cardiac fibroblasts adopt an endothelial cell phenotype after acute ischemic injury via activation of the p53 pathway, which translated into improved cardiac function in a murine model of cardiac injury. The formation of functional vessels was not reported. In direct contrast to these findings, He et al[47] used genetic lineage tracing with pulse-chase labeling to show that pre-existing endothelial cells rather than fibroblasts form new vessels in a murine model of myocardial infarction. This finding challenged the premise that MSC-endothelial transition (MEndoT) contributes to vasculogenesis in vivo. Several immature MSCs, however, have more recently been identified to differentiate into vascular lineages and contribute to neovascularization, including hemangioma stem cells (HemSCs)[48–50] and very small embryonic-like stem cells.[51,52] These cells are multipotent and have the ability

Figure 3 Continued. Anti-CD31 immunofluorescence staining (Alexa Fluor 647), merged signal from GFP and AF647 Anti-CD31. Scale bars=100 µm. **D**, Immunofluorescence staining of VWF (von Willebrand factor). From left to right, GFP signal from transplanted cells, anti-VWF immunofluorescence staining (Alexa Fluor 647), merged signal from GFP and AF647 anti-VWF staining. Scale bars=100 µm. **E**, Transplantation of single VSPC1 cell populations from Actin-RFP (n=6), single VSPC2 cell populations from GFP mice (n=6), and the combination of VSPC1 Actin-RFP cells and VSPC2 Actin-GFP cells (1:1 ratio; n=6). Scale bars=100 µm. **F**, A bar graph comparing the differentiation capacity of VSPC1, VSPC2, and VSPC1+VSPC2 combination after transplantation. **G**, Experimental schematic for in vivo rescue experiments. A total number of 500 000 VSPC1, VSPC2 or VSPC1+VSPC2 (1:1 ratio) GFP+ cells were injected with GFR Matrigel and compared with the injection of GFR Matrigel alone. Blood flow was monitored following ligation of the femoral artery using laser Doppler imaging. Diagram was created with Biorender. **H**, Laser Doppler measurement of restored blood flow in ischemic hindlimbs of immunodeficient Rag2/gamma(c) knockout mice treated with transplanted cells. Red and orange areas indicate high blood flow, while blue or black areas indicate decreased blood flow. **I**, Quantification of blood flow in the presence of an injection of GFR Matrigel only (n=6) compared with injection of VSPC1 cells only (n=6), VSPC2 cells only (n=6), or VSPC1+VSPC2 cotransplant (n=6), at day 0, 7, 14, and 28 post-transplantation. Significance was determined by comparing the indicated group with VSPC1+VSPC2 cotransplant group. **J**, Fluorescence microscopy demonstrates cotransplantation of Actin-GFP mice derived VSPC1 and VSPC2 cell populations in vivo yields GFP vessels carrying blood in the ischemic hindlimb 14 days after transplantation. Scale bars=100 µm. **K**, Perfusion of vessels with DyLight 649-lectin demonstrates functionality. Scale bars=100 µm. **L**, A bar graph comparing GFP+ vessels per view (n=10). **M**, A bar graph comparing Lectin+ percentage of GFP+ vessels (n=10).

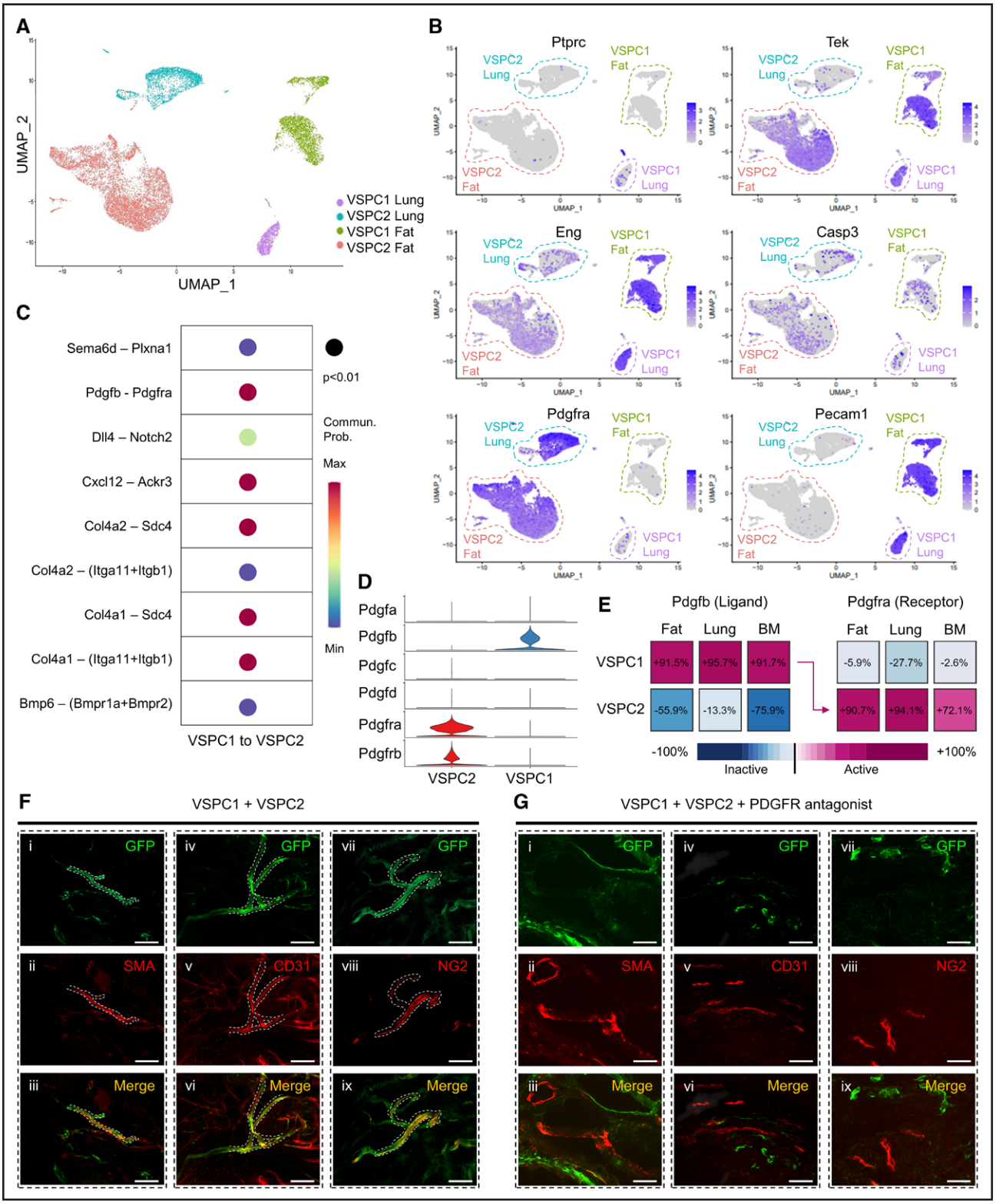

Figure 4. Regulatory crosstalk between VSPC1 (P1) and VSPC2 (P2) in promotion of neovascularization.
A, Single-cell RNA-sequencing data of VSPC1 and VSPC2 from mouse fat and lung tissues are shown by uniform manifold approximation and projection (UMAP). **B**, Representative gene expression of VSPC1 and VSPC2 populations. **C** and **D**, CellChat analysis of VSPC1 to VSPC2 interactions revealed PDGF signal from VSPC1 cells is a potential regulator of VSPC2 cell differentiation. **E**, Microarray data of VSPC1 and VSPC2 populations from fat, lung, and bone marrow showed specific ligand-receptor expression patterns between VSPC1 and VSPC2. **F** and **G**, Co-injection of GFP (green fluorescent protein) VSPC1 and GFP VSPC2 cell populations into the fat pad of immunodeficient Rag2/gamma(c) knockout mice (n=5) with or without a saturating dose of PDGFR antagonist. Vessel markers, including smooth muscle (SMA; i-iii), endothelial (CD31; iv-vi), and pericyte (NG2; vii-ix) have been tested. Scale bars=100 μm.

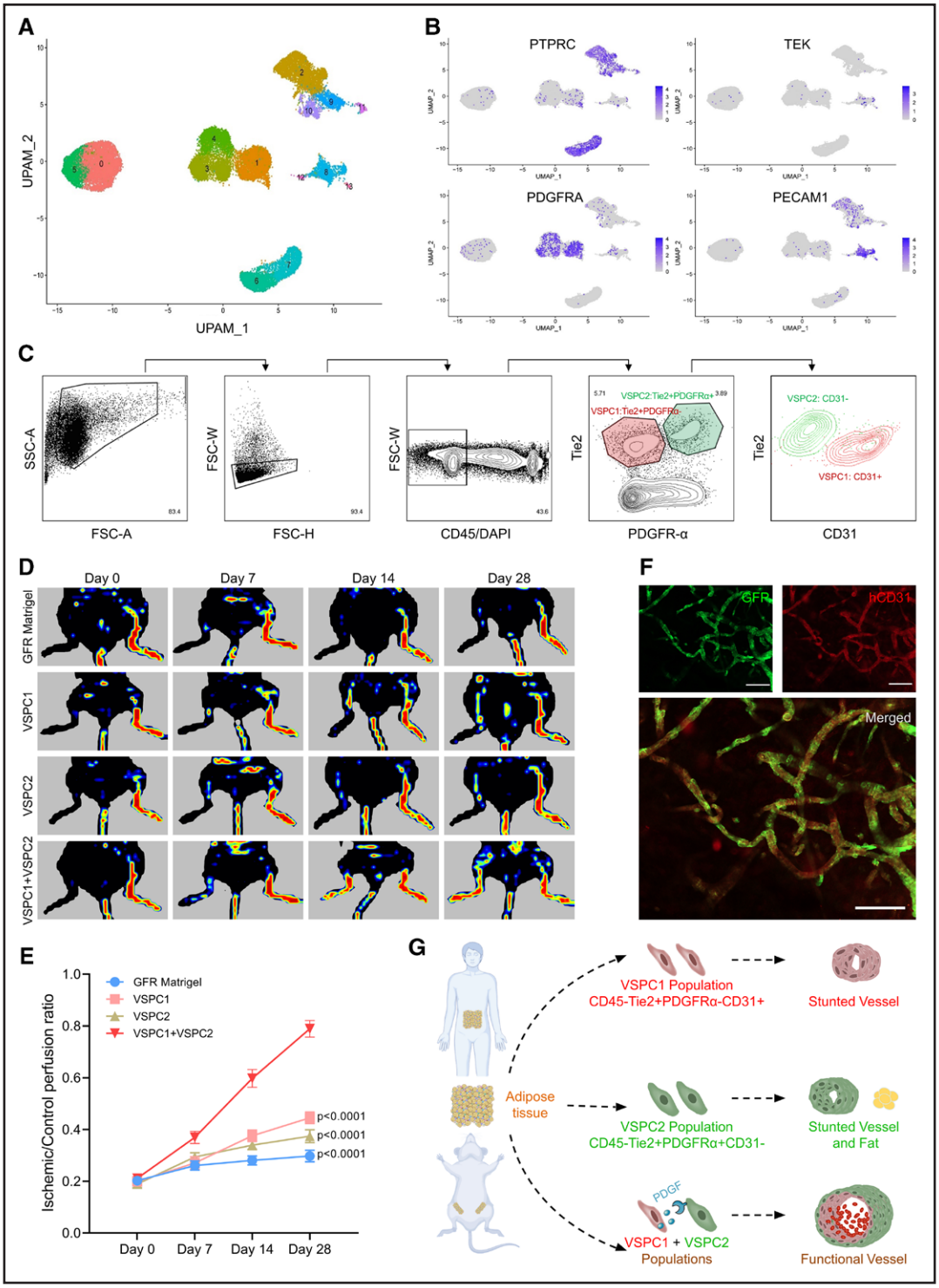

Figure 5. Human lipoaspirate contains functional, analogous VSPC1 (P1) and VSPC2 (P2) populations.
A, Single-cell RNA-sequencing data of human adipose stromal vascular fraction shown by uniform manifold approximation and projection. **B**, Representative gene expression of VSPC1 and VSPC2 populations. **C**, Prospective isolation of transcriptionally similar cell subsets of VSPC1 and VSPC2 from human adipose tissue. **D**, Cotransplantation of VSPC1 and VSPC2 populations were tested with immunodeficient Rag2/gamma(c) knockout mice. Laser Doppler measurement and quantification of restored blood flow in ischemic hindlimbs of immunodeficient Rag2/gamma(c) knockout mice treated with transplanted growth factor reduced (GFR) Matrigel or GFR Matrigel plus human derived cells. Red and orange areas indicate high blood flow, while blue or black areas indicate decreased blood flow. **E**, Quantification of blood flow in the presence of an injection of GFR Matrigel only (n=6) compared with injection of VSPC1 cells only (n=6), VSPC2 cells only (n=6), or VSPC1+VSPC2 cotransplant (n=6), at day 0, 7, 14, and 28 post-transplantation. Significance was determined by comparing the indicated group with VSPC1+VSPC2 cotransplant group. **F**, Overlapping of GFP-labeled human VSPC1+VSPC2 cells with Anti-hCD31 immunofluorescence staining (Alexa Fluor 647). Scale bars=100 μm. **G**, Diagram to show the properties of VSPC1 and VSPC2 vessel-forming progenitors and their interactions. Diagram was created with Biorender.

of differentiating into endothelial cells, adipocytes, and osteoblast. In this study, we used a multicolor lineage tracing reporter system that enables clear identification of subpopulations of MSCs (VSPC1 and VSPC2) that can form de novo vessels when cotransplanted after ischemic injury. Aside from blood vessel and adipocyte fates, we do not observe lineage commitment in vivo by VSPC1 and VSPC2 to other mesenchymal fates such as osteoblast. We provide further support for the MSC-endothelial transition by demonstrating that cotransplantation of subpopulations of MSCs expressing Tie2 (VSPC1 and VSPC2) formed functional vessels in vivo and provided sufficient perfusion to rescue the hind limbs of mice after femoral artery ligation.

The importance of Tie2 and Sca1 in vasculogenesis has been reported previously. Tie2 is a transmembrane tyrosine-protein kinase receptor that binds angiopoietin, mediating signaling pathways that regulate embryonic vascular development. Although it is presumed that Tie2's effect on angiogenesis is primarily exerted by its expression on endothelial cells, recent data has shown that monocytes[53,54] and pericytes[53] express functional Tie2 receptors. In patients with critical limb ischemia, Patel et al[54] showed that Tie2-expressing monocytes/macrophages were 10-fold more abundant before revascularization and were required for normal endothelial tube formation in vitro and in vivo. In contrast, Teichert et al[55] found that the presence of Tie2 in pericytes limited endothelial sprouting. In MSCs, Tie2 expression separates MSC lineages into those that can form vessels and adipocytes from those that can form bone.[14] Taken together, it appears that Tie2 is a regulator of vasculogenesis across multiple cell types. Sca1-expressing progenitor cells have been reported to respond to injury and give rise to vascular endothelial cells and smooth muscle cells.[56–58] The multipotential and heterogeneity of Sca1-expressing cells have also been observed in our transplantation study.

Although both MSC subpopulation VSPC1 and VSPC2 expressed Tie2 and Sca1, they differed in their expression of CD31, PDGFRα, CD105. Anderson et al[59] also showed that MSCs are heterogenous for the expression of CD105, a member of the TGF-β family. We found that the subpopulation of MSCs with low CD105 expression (VSPC2) have greater potential to differentiate into adipocytes likely because of their reduced responsiveness to TGF-β/smad2 signaling, which is consistent with previous studies.[60] Interestingly, MSCs with low CD105 expression (VSPC2) have high mRNA levels PDGF receptors, whereas those with high CD105 expression (VSPC1) have high mRNA levels of PDGF ligands, suggesting crosstalk between these 2 cell subpopulations. Like TGF-β, PDGF signaling has been found to play an important role the differentiation of MSCs into adipocytes,[61] which may explain why cotransplantation of the 2 subpopulations of VSPC1 and VSPC2 was required to inhibit adipogenesis and favor vessel formation in vitro and in vivo. Importantly, the activation of the PDGFα receptor also promotes angiogenesis,[62,63] providing further support for the cotransplantation of these cell subpopulations. Spatial transcriptomics should be considered to further characterize cell surface markers and cell-cell interactions further in VSPC1 and VSPC2.

In summary, transplantation of distinct MSC subpopulations VSPC1 and VSPC2 can promote neovasculogenesis for the treatment of ischemic diseases. Because MSCs may be better tolerated than other cell types due to their immunomodulatory properties,[64] allogenic transplantation may be feasible, enabling "off the shelf" therapy. While the differentiation of pluripotent stem cell populations into vessel lineages is another strategy, it requires in vitro culture and is associated with significant immunogenic[65] and tumorigenic risks.[66] Thus, the enrichment of a specific combination of VSPC1 and VSPC2 vessel-forming progenitor populations from a suitable source such as adipose tissue followed by direct transplantation may present an effective method for inducing formation of new blood vessels for treatment of ischemic injury.

ARTICLE INFORMATION

Received December 10, 2021; accepted March 28, 2023.

Affiliations

Institute for Stem Cell Biology and Regenerative Medicine (L.Z., Y.W., R.C.R., X.Z., C.M., H.M.S., L.S.K., M.R.B., R.E.B., L.Y.L., T.H.A., R.S., M.Y.H., I.L.W., J.C.W., M.T.L., C.K.F.C.), Department of Surgery, Division of Plastic and Reconstructive Surgery (L.Z., Y.W., R.C.R., C.M., H.M.S., L.S.K., M.R.B., L.L.Y.L., T.H.A., D.C.W., M.T.L., C.K.F.C.), Stanford Cardiovascular Institute (K.S., J.S., X.Z., X.H., J.C.W., M.T.L., P.K.N., C.K.F.C.), Department of Medicine, Division of Cardiovascular Medicine (K.S., J.S., X.Z., X.H., J.C.W., P.K.N.), and Department of Developmental Biology (I.L.W., C.K.F.C.), Stanford University School of Medicine, CA. Department of Orthopaedic Surgery, Tongji Hospital, Tongji Medical College, Huazhong University of Science and Technology, Wuhan, China (L.Z., Y.W., J.X.). School of Chemical Biology and Biotechnology, Peking University Shenzhen Graduate School, China (A.S.L.). Institute for Cancer Research, Shenzhen Bay Laboratory, China (A.S.L.). Center for Integrative Medical Sciences and Advanced Data Science Project, RIKEN, Tokyo, Japan (J.S.).

Author Contributions

C.K.F. Chan, L. Zhao, and A.S. Lee designed this study. C.K.F. Chan, L. Zhao, A.S. Lee, Y. Wang, R.C. Ransom, X. Zhao, C. Ma, H.M. Steininger, L.S. Koepke, M.R. Borrelli, R.E. Brewer, L.L.Y. Lee, and X. Huang performed experiments. K. Sasagawa, J. Sokol, T.H. Ambrosi, R. Sinha, M.Y. Hoover, and J. Seita performed RNA sequencing and data analysis. I.L. Weissman, J.C. Wu, D.C. Wan, J. Xiao, M.T. Longaker, P.K. Nguyen, and C.K.F. Chan supervised the project. C.K.F. Chan, L. Zhao, and A.S. Lee prepared the article. All authors reviewed and approved the article.

Sources of Funding

This study was supported by National Institutes of Health (NIH; R01DE021683, K99-R00AG049958, S10OD028493, R01DE026730, R01DE027323, R01DK115600, R21DE024230, R01DE019434, RC2DE020771, U01HL099776, R21DE019274, U01HL099999, R01CA86065, R01HL058770, R01HL134830), Siebel Fellowship, Prostate Cancer Foundation Young Investigator Award, Stinehart/Reed Award, the Heritage Medical Foundation, Wu Tsai Human Performance Alliance, Stanford CVI Seed Grant, Arthritis National Research Foundation, California Institute for Regenerative Medicine, the American Federation for Aging Research, Chan Zuckerberg Biohub, gift from Roger Silk, gift from LDVP, endowment from the DiGenova Family, Hagey Laboratory for Pediatric Regenerative Medicine, and the Gunn/Olivier Research Fund.

Disclosures

None.

Supplemental Material

Figures S1–S5
Major Resources Table

REFERENCES

1. Morley RL, Sharma A, Horsch AD, Hinchliffe RJ. Peripheral artery disease. *BMJ*. 2018;360:j5842. doi: 10.1136/bmj.j5842
2. Song P, Rudan D, Zhu Y, Fowkes FJI, Rahimi K, Fowkes FGR, Rudan I. Global, regional, and national prevalence and risk factors for peripheral artery disease in 2015: an updated systematic review and analysis. *Lancet Glob Health*. 2019;7:e1020–e1030. doi: 10.1016/S2214-109X(19)30255-4
3. Lee SH, Wolf PL, Escudero R, Deutsch R, Jamieson SW, Thistlethwaite PA. Early expression of angiogenesis factors in acute myocardial ischemia and infarction. *N Engl J Med*. 2000;342:626–633. doi: 10.1056/nejm200003023420904
4. Mills JD, Fischer D, Villanueva FS. Coronary collateral development during chronic ischemia: serial assessment using harmonic myocardial contrast echocardiography. *J Am Coll Cardiol*. 2000;36:618–624. doi: 10.1016/s0735-1097(00)00739-7
5. Giacca M, Zacchigna S. VEGF gene therapy: therapeutic angiogenesis in the clinic and beyond. *Gene Ther*. 2012;19:622–629. doi: 10.1038/gt.2012.17
6. Domouzoglou EM, Naka KK, Vlahos AP, Papafaklis MI, Michalis LK, Tsatsoulis A, Maratos-Flier E. Fibroblast growth factors in cardiovascular disease: the emerging role of FGF21. *Am J Physiol Heart Circ Physiol*. 2015;309:H1029–H1038. doi: 10.1152/ajpheart.00527.2015
7. Jay SM, Lee RT. Protein engineering for cardiovascular therapeutics: untapped potential for cardiac repair. *Circ Res*. 2013;113:933–943. doi: 10.1161/CIRCRESAHA.113.300215
8. Nguyen PK, Rhee JW, Wu JC. Adult Stem cell therapy and heart failure, 2000 to 2016: a systematic review. *JAMA Cardiol*. 2016;1:831–841. doi: 10.1001/jamacardio.2016.2225
9. Mathur A, Fernandez-Aviles F, Dimmeler S, Hauskeller C, Janssens S, Menasche P, Wojakowski W, Martin JF, Zeiher A; BAMI Investigators. The consensus of the task force of the European society of cardiology concerning the clinical investigation of the use of autologous adult stem cells for the treatment of acute myocardial infarction and heart failure: update 2016. *Eur Heart J*. 2017;38:2930–2935. doi: 10.1093/eurheartj/ehw640
10. Tachibana A, Santoso MR, Mahmoudi M, Shukla P, Wang L, Bennett M, Goldstone AB, Wang M, Fukushi M, Ebert AD, et al. Paracrine effects of the pluripotent stem cell-derived cardiac myocytes salvage the injured myocardium. *Circ Res*. 2017;121:e22–e36. doi: 10.1161/CIRCRESAHA.117.310803
11. Crisan M, Yap S, Casteilla L, Chen C-W, Corselli M, Park TS, Andriolo G, Sun B, Zheng B, Zhang L, et al. A perivascular origin for mesenchymal stem cells in multiple human organs. *Cell Stem Cell*. 2008;3:301–313. doi: 10.1016/j.stem.2008.07.003
12. Cano E, Gebala V, Gerhardt H. Pericytes or mesenchymal stem cells: is that the question?. *Cell Stem Cell*. 2017;20:296–297. doi: 10.1016/j.stem.2017.02.005
13. Bianco P, Cao X, Frenette PS, Mao JJ, Robey PG, Simmons PJ, Wang CY. The meaning, the sense and the significance: translating the science of mesenchymal stem cells into medicine. *Nat Med*. 2013;19:35–42. doi: 10.1038/nm.3028
14. Chan CKF, Lindau P, Jiang W, Chen JY, Zhang LF, Chen C-C, Seita J, Sahoo D, Kim J-B, Lee A, et al. Clonal precursor of bone, cartilage, and hematopoietic niche stromal cells. *Proc Natl Acad Sci USA*. 2013;110:12643–12648. doi: 10.1073/pnas.1310212110
15. Fang JS, Dai C, Kurjiaka DT, Burt JM, Hirschi KK. Connexin45 regulates endothelial-induced mesenchymal cell differentiation toward a mural cell phenotype. *Arterioscler Thromb Vasc Biol*. 2013;33:362–368. doi: 10.1161/ATVBAHA.112.255950
16. Janeczek Portalska K, Leferink A, Groen N, Fernandes H, Moroni L, van Blitterswijk C, de Boer J. Endothelial differentiation of mesenchymal stromal cells. *PLoS One*. 2012;7:e46842. doi: 10.1371/journal.pone.0046842
17. Yu QC, Song W, Wang D, Zeng YA. Identification of blood vascular endothelial stem cells by the expression of protein C receptor. *Cell Res*. 2016;26:1079–1098. doi: 10.1038/cr.2016.85
18. Wakabayashi T, Naito H, Suehiro JI, Lin Y, Kawaji H, Iba T, Kouno T, Ishikawa-Kato S, Furuno M, Takara K, et al. CD157 marks tissue-resident endothelial stem cells with homeostatic and regenerative properties. *Cell Stem Cell*. 2018;22:384–397.e6. doi: 10.1016/j.stem.2018.01.010
19. Bautch VL. Stem cells and the vasculature. *Nat Med*. 2011;17:1437–1443. doi: 10.1038/nm.2539
20. Wang D, Li LK, Dai T, Wang A, Li S. Adult stem cells in vascular remodeling. *Theranostics*. 2018;8:815–829. doi: 10.7150/thno.19577
21. Yoder MC. Endothelial stem and progenitor cells (stem cells): (2017 Grover Conference Series). *Pulm Circ*. 2018;8:2045893217743950. doi: 10.1177/2045893217743950
22. Ueno H, Weissman IL. Clonal analysis of mouse development reveals a polyclonal origin for yolk sac blood islands. *Dev Cell*. 2006;11:519–533. doi: 10.1016/j.devcel.2006.08.001
23. Rinkevich Y, Lindau P, Ueno H, Longaker MT, Weissman IL. Germ-layer and lineage-restricted stem/progenitors regenerate the mouse digit tip. *Nature*. 2011;476:409–413. doi: 10.1038/nature10346
24. Tang J, Wang H, Huang X, Li F, Zhu H, Li Y, He L, Zhang H, Pu W, Liu K, et al. Arterial sca1(+) vascular stem cells generate de novo smooth muscle for artery repair and regeneration. *Cell Stem Cell*. 2019;26:81–96. doi: 10.1016/j.stem.2019.11.010
25. Rinkevich Y, Montoro DT, Contreras-Trujillo H, Harari-Steinberg O, Newman AM, Tsai JM, Lim X, Van-Amerongen R, Bowman A, Januszyk M, et al. In vivo clonal analysis reveals lineage-restricted progenitor characteristics in mammalian kidney development, maintenance, and regeneration. *Cell Rep*. 2014;7:1270–1283. doi: 10.1016/j.celrep.2014.04.018
26. Chan CKF, Seo EY, Chen JY, Lo D, McArdle A, Sinha R, Tevlin R, Seita J, Vincent-Tompkins J, Wearda T, et al. Identification and specification of the mouse skeletal stem cell. *Cell*. 2015;160:285–298. doi: 10.1016/j.cell.2014.12.002
27. Ransom RC, Carter AC, Salhotra A, Leavitt T, Marecic O, Murphy MP, Lopez ML, Wei Y, Marshall CD, Shen EZ, et al. Mechanoresponsive stem cells acquire neural crest fate in jaw regeneration. *Nature*. 2018;563:514–521. doi: 10.1038/s41586-018-0650-9
28. Losordo DW, Isner JM. Estrogen and angiogenesis: a review. *Arterioscler Thromb Vasc Biol*. 2001;21:6–12. doi: 10.1161/01.atv.21.1.6
29. Barnabas O, Wang H, Gao XM. Role of estrogen in angiogenesis in cardiovascular diseases. *J Geriatr Cardiol*. 2013;10:377–382. doi: 10.3969/j.issn.1671-5411.2013.04.008
30. Sparrow CP, Burton CA, Hernandez M, Mundt S, Hassing H, Patel S, Rosa R, Hermanowski-Vosatka A, Wang PR, Zhang D, et al. Simvastatin has anti-inflammatory and antiatherosclerotic activities independent of plasma cholesterol lowering. *Arterioscler Thromb Vasc Biol*. 2001;21:115–121. doi: 10.1161/01.atv.21.1.115
31. Stuart T, Butler A, Hoffman P, Hafemeister C, Papalexi E, Mauck WM, Hao Y, Stoeckius M, Smibert P, Satija R. Comprehensive integration of single-cell data. *Cell*. 2019;177:1888–1902.e21. doi: 10.1016/j.cell.2019.05.031
32. Jin S, Guerrero-Juarez CF, Zhang L, Chang I, Ramos R, Kuan CH, Myung P, Plikus MV, Nie Q. Inference and analysis of cell-cell communication using CellChat. *Nat Commun*. 2021;12:1088. doi: 10.1038/s41467-021-21246-9
33. Seita J, Sahoo D, Rossi DJ, Bhattacharya D, Serwold T, Inlay MA, Ehrlich LIR, Fathman JW, Dill DL, Weissman IL. Gene expression commons: an open platform for absolute gene expression profiling. *PLoS One*. 2012;7:e40321. doi: 10.1371/journal.pone.0040321
34. Niiyama H, Huang NF, Rollins MD, Cooke JP. Murine model of hindlimb ischemia. *J Vis Exp*. 2009;23:1035. doi: 10.3791/1035
35. Galasso G, De Rosa R, Ciccarelli M, Sorriento D, Del Giudice C, Strisciuglio T, De Biase C, Luciano R, Piccolo R, Pierri A, et al. beta2-Adrenergic receptor stimulation improves endothelial progenitor cell-mediated ischemic neoangiogenesis. *Circ Res*. 2013;112:1026–1034. doi: 10.1161/CIRCRESAHA.111.300152
36. Ii M, Nishimura H, Iwakura A, Wecker A, Eaton E, Asahara T, Losordo DW. Endothelial progenitor cells are rapidly recruited to myocardium and mediate protective effect of ischemic preconditioning via "imported" nitric oxide synthase activity. *Circulation*. 2005;111:1114–1120. doi: 10.1161/01.CIR.0000157144.24888.7E
37. Farbehi N, Patrick R, Dorison A, Xaymardan M, Janbandhu V, Wystub-Lis K, Ho JW, Nordon RE, Harvey RP. Single-cell expression profiling reveals dynamic flux of cardiac stromal, vascular and immune cells in health and injury. *Elife*. 2019;8:e43882. doi: 10.7554/eLife.43882
38. Hare JM, Fishman JE, Gerstenblith G, DiFede Velazquez DL, Zambrano JP, Suncion VY, Tracy M, Ghersin E, Johnston PV, Brinker JA, et al. Comparison of allogeneic vs autologous bone marrow-derived mesenchymal stem cells delivered by transendocardial injection in patients with ischemic cardiomyopathy: the POSEIDON randomized trial. *JAMA*. 2012;308:2369–2379. doi: 10.1001/jama.2012.25321

39. Ascheim DD, Gelijns AC, Goldstein D, Moye LA, Smedira N, Lee S, Klodell CT, Szady A, Parides MK, Jeffries NO, et al. Mesenchymal precursor cells as adjunctive therapy in recipients of contemporary left ventricular assist devices. *Circulation*. 2014;129:2287–2296. doi: 10.1161/CIRCULATIONAHA.113.007412
40. Prasad K, Sharma A, Garg A, Mohanty S, Bhatnagar S, Johri S, Singh KK, Nair V, Sarkar RS, Gorthi SP, et al; InveST Study Group. Intravenous autologous bone marrow mononuclear stem cell therapy for ischemic stroke: a multicentric, randomized trial. *Stroke*. 2014;45:3618–3624. doi: 10.1161/STROKEAHA.114.007028
41. Kim J, Wu Q, Zhang Y, Wiens KM, Huang Y, Rubin N, Shimada H, Handin RI, Chao MY, Tuan T-L, et al. PDGF signaling is required for epicardial function and blood vessel formation in regenerating zebrafish hearts. *Proc Natl Acad Sci USA*. 2010;107:17206–17210. doi: 10.1073/pnas.0915016107
42. Tang W, Zeve D, Suh JM, Bosnakovski D, Kyba M, Hammer RE, Tallquist MD, Graff JM. White fat progenitor cells reside in the adipose vasculature. *Science*. 2008;322:583–586. doi: 10.1126/science.1156232
43. Vijay J, Gauthier MF, Biswell RL, Louiselle DA, Johnston JJ, Cheung WA, Belden B, Pramatarova A, Biertho L, Gibson M, et al. Single-cell analysis of human adipose tissue identifies depot and disease specific cell types. *Nat Metab*. 2020;2:97–109. doi: 10.1038/s42255-019-0152-6
44. Bianco P. "Mesenchymal" stem cells. *Annu Rev Cell Dev Biol*. 2014;30:677–704. doi: 10.1146/annurev-cellbio-100913-013132
45. Trounson A, McDonald C. Stem cell therapies in clinical trials: progress and challenges. *Cell Stem Cell*. 2015;17:11–22. doi: 10.1016/j.stem.2015.06.007
46. Ubil E, Duan J, Pillai IC, Rosa-Garrido M, Wu Y, Bargiacchi F, Lu Y, Stanbouly S, Huang J, Rojas M, et al. Mesenchymal-endothelial transition contributes to cardiac neovascularization. *Nature*. 2014;514:585–590. doi: 10.1038/nature13839
47. He L, Huang X, Kanisicak O, Li Y, Wang Y, Li Y, Pu W, Liu Q, Zhang H, Tian X, et al. Preexisting endothelial cells mediate cardiac neovascularization after injury. *J Clin Investig*. 2017;127:2968–2981. doi: 10.1172/jci93868
48. Khan ZA, Boscolo E, Picard A, Psutka S, Melero-Martin JM, Bartch TC, Mulliken JB, Bischoff J. Multipotential stem cells recapitulate human infantile hemangioma in immunodeficient mice. *J Clin Investig*. 2008;118:2592–2599. doi: 10.1172/JCI33493
49. Boscolo E, Mulliken JB, Bischoff J. VEGFR-1 mediates endothelial differentiation and formation of blood vessels in a murine model of infantile hemangioma. *Am J Pathol*. 2011;179:2266–2277. doi: 10.1016/j.ajpath.2011.07.040
50. Boscolo E, Stewart CL, Greenberger S, Wu JK, Durham JT, Herman IM, Mulliken JB, Kitajewski J, Bischoff J. JAGGED1 signaling regulates hemangioma stem cell-to-pericyte/vascular smooth muscle cell differentiation. *Arterioscler Thromb Vasc Biol*. 2011;31:2181–2192. doi: 10.1161/ATVBAHA.111.232934
51. Guerin CL, Loyer X, Vilar J, Cras A, Mirault T, Gaussem P, Silvestre JS, Smadja DM. Bone-marrow-derived very small embryonic-like stem cells in patients with critical leg ischaemia: evidence of vasculogenic potential. *Thromb Haemost*. 2015;113:1084–1094. doi: 10.1160/TH14-09-0748
52. Guerin CL, Rossi E, Saubamea B, Cras A, Mignon V, Silvestre JS, Smadja DM. Human very small embryonic-like cells support vascular maturation and therapeutic revascularization induced by endothelial progenitor cells. *Stem Cell Rev Rep*. 2017;13:552–560. doi: 10.1007/s12015-017-9731-7
53. De Palma M, Venneri MA, Galli R, Sergi Sergi L, Politi LS, Sampaolesi M, Naldini L. Tie2 identifies a hematopoietic lineage of proangiogenic monocytes required for tumor vessel formation and a mesenchymal population of pericyte progenitors. *Cancer Cell*. 2005;8:211–226. doi: 10.1016/j.ccr.2005.08.002
54. Patel AS, Smith A, Nucera S, Biziato D, Saha P, Attia RQ, Humphries J, Mattock K, Grover SP, Lyons OT, et al. TIE2-expressing monocytes/macrophages regulate revascularization of the ischemic limb. *EMBO Mol Med*. 2013;5:858–869. doi: 10.1002/emmm.201302752
55. Teichert M, Milde L, Holm A, Stanicek L, Gengenbacher N, Savant S, Ruckdeschel T, Hasanov Z, Srivastava K, Hu J, et al. Pericyte-expressed Tie2 controls angiogenesis and vessel maturation. *Nat Commun*. 2017;8:16106. doi: 10.1038/ncomms16106
56. Tang J, Zhu H, Liu S, Wang H, Huang X, Yan Y, Wang L, Zhou B. Sca1 marks a reserve endothelial progenitor population that preferentially expand after injury. *Cell Discov*. 2021;7:88. doi: 10.1038/s41421-021-00303-z
57. Vagnozzi RJ, Sargent MA, Lin SJ, Palpant NJ, Murry CE, Molkentin JD. Genetic lineage tracing of sca-1(+) cells reveals endothelial but not myogenic contribution to the murine heart. *Circulation*. 2018;138:2931–2939. doi: 10.1161/CIRCULATIONAHA.118.035210
58. Tang J, Wang H, Huang X, Li F, Zhu H, Li Y, He L, Zhang H, Pu W, Liu K, et al. Arterial sca1(+) vascular stem cells generate de novo smooth muscle for artery repair and regeneration. *Cell Stem Cell*. 2020;26:81–96.e4. doi: 10.1016/j.stem.2019.11.010
59. Anderson P, Carrillo-Galvez AB, Garcia-Perez A, Cobo M, Martin F. CD105 (endoglin)-negative murine mesenchymal stromal cells define a new multipotent subpopulation with distinct differentiation and immunomodulatory capacities. *PLoS One*. 2013;8:e76979. doi: 10.1371/journal.pone.0076979
60. Young K, Conley B, Romero D, Tweedie E, O'Neill C, Pinz I, Brogan L, Lindner V, Liaw L, Vary CPH. BMP9 regulates endoglin-dependent chemokine responses in endothelial cells. *Blood*. 2012;120:4263–4273. doi: 10.1182/blood-2012-07-440784
61. Ng F, Boucher S, Koh S, Sastry KSR, Chase L, Lakshmipathy U, Choong C, Yang Z, Vemuri MC, Rao MS, et al. PDGF, TGF-beta, and FGF signaling is important for differentiation and growth of mesenchymal stem cells (MSCs): transcriptional profiling can identify markers and signaling pathways important in differentiation of MSCs into adipogenic, chondrogenic, and osteogenic lineages. *Blood*. 2008;112:295–307. doi: 10.1182/blood-2007-07-103697
62. Gomes SA, Rangel EB, Premer C, Dulce RA, Cao Y, Florea V, Balkan W, Rodrigues CO, Schally AV, Hare JM. S-nitrosoglutathione reductase (GSNOR) enhances vasculogenesis by mesenchymal stem cells. *Proc Natl Acad Sci USA*. 2013;110:2834–2839. doi: 10.1073/pnas.1220185110
63. Zhang J, Cao R, Zhang Y, Jia T, Cao Y, Wahlberg E. Differential roles of PDGFR-alpha and PDGFR-beta in angiogenesis and vessel stability. *FASEB J*. 2009;23:153–163. doi: 10.1096/fj.08-113860
64. Ankrum JA, Ong JF, Karp JM. Mesenchymal stem cells: immune evasive, not immune privileged. *Nat Biotechnol*. 2014;32:252–260. doi: 10.1038/nbt.2816
65. Zhao T, Zhang ZN, Rong Z, Xu Y. Immunogenicity of induced pluripotent stem cells. *Nature*. 2011;474:212–215. doi: 10.1038/nature10135
66. Nguyen PK, Neofytou E, Rhee JW, Wu JC. Potential strategies to address the major clinical barriers facing stem cell regenerative therapy for cardiovascular disease: a review. *JAMA Cardiol*. 2016;1:953–962. doi: 10.1001/jamacardio.2016.2750